Educational Administration: Theory and Practice
2023, 29(4), 1275-1287
ISSN: 2148-2403
https://kuey.net/ **Research Article**

Transformer-Less Grid-Connected Photovoltaic Inverter

Repalle Rohit[1*], Gudipati Kishor[2]

[1*]Research Scholar, EEE Department, Jawaharlal Nehru Technological University Anantapur, Ananthapuramu & G. Pulla Reddy Engineering College Kurnool, affiliated to Jawaharlal Nehru Technological University Anantapur, Ananthapuramu, repallerohit@gmail.com
[2]Professor, EEE Department, G. Pulla Reddy Engineering College Kurnool, Affiliated to Jawaharlal Nehru Technological University Anantapur, Ananthapuramu, gudipatikishor@gmail.com

***Corresponding Author:** Repalle Rohit
*Research Scholar, EEE Department, Jawaharlal Nehru Technological University Anantapur, Ananthapuramu & G. Pulla Reddy Engineering College Kurnool, affiliated to Jawaharlal Nehru Technological University Anantapur, Ananthapuramu, repallerohit@gmail.com

Citation: Repalle Rohit , et al (2023), Transformer-Less Grid-Connected Photovoltaic Inverter, *Educational Administration: Theory and Practice*, 29(4), 1275-1287, Doi: 10.53555/kuey.v29i4.4151

ARTICLE INFO **ABSTRACT**

The increasing use of inverters in microgrids and Photovoltaic generation systems has made it more crucial than ever to achieve low-distortion, high-quality power export from inverters. The presence of harmonics in the grid's pre-existing voltage/current distortion will result in poor power quality. A well-designed inverter impacts minimizing the percentage of total harmonic distortion (THD) in the power supplied to the grid. This paper proposes H6 inverter topology in comparison with conventional H4(Full-bridge) topology to reduce the grid disturbance in the context of THD and maintain good waveform quality. The Transformer-less Single-Phase Grid-Connected photovoltaic inverter using MATLAB/Simulation is implemented. The depreciation of %THD and improvement in the power factor in the proposed system emphasize its prominence in practical implementation.

Keywords: total harmonic distortion, inverters, photovoltaic (PV) systems.

I. INTRODUCTION

Solar power systems and other renewable energy sources have experienced steady growth in global electrical energy production. The utilization of solar photovoltaic (PV) systems for generating electricity is on the rise, driven by decreasing installation costs, rendering it a competitive option among sustainable energy solutions [1]. Anticipating the grid integration of multiple small inverters (less than 50 kW) with specific features is feasible for PV systems. However, existing standards and guidelines for grid-connected generators were developed before the widespread adoption of small-scale systems employing power-electronic interfaces. Researchers and Distribution network operators (DNOs) researchers in the field highlight power factor characteristics and harmonic distortion as pressing concerns requiring immediate attention. Harmonic distortion poses particular risks to distribution losses and potential disruptions to other consumers on the network when power-electronic sources operate in parallel, two distinct effects, attenuation, and cancellation, impact harmonic generation (refer to [2] and [3]).
Network service providers often prioritize the power factor of sources and loads because it impacts losses. Many commercial inverters designed for grid-connected small generators are engineered to operate at a unity power factor. This concern affects equipment manufacturers, utility companies, and distribution network operators (DNOs).
Numerous national and international organizations are actively involved in developing standards for electrical supply systems. In the USA, such organizations include the IEEE; in the UK, the British Standards Institution (BSI) and the Electricity Association; and internationally, the IEC. These collective efforts have created two draft Standards to date: IEEE P1547/D10 [4] and G83 [5].
This paper proposes an H6 grid-connected photovoltaic inverter, a simple LCL filter has traditionally been utilized. The impetus of this research is to rate the impact of the H6 inverter topology on the overall working of a photovoltaic system connected to the grid. A single DC-link decoupling capacitor is incorporated into the H6

inverter to improve the circuit reliability. In section II system configuration is provided with a detailed explanation. In Section III two types of inverter topologies and their respective modes of operation are presented. Section IV consists of a phase-locked loop. Section V consists of Grid Requirements and Standards. Section VI provides the parameters of the system. Section VII provides simulation results and discussion. Section VIII provides tables and graphs that signify the performance of the overall system. Section IX concludes the hypotheses followed by the referred citations.

II. SYSTEM CONFIGURATION

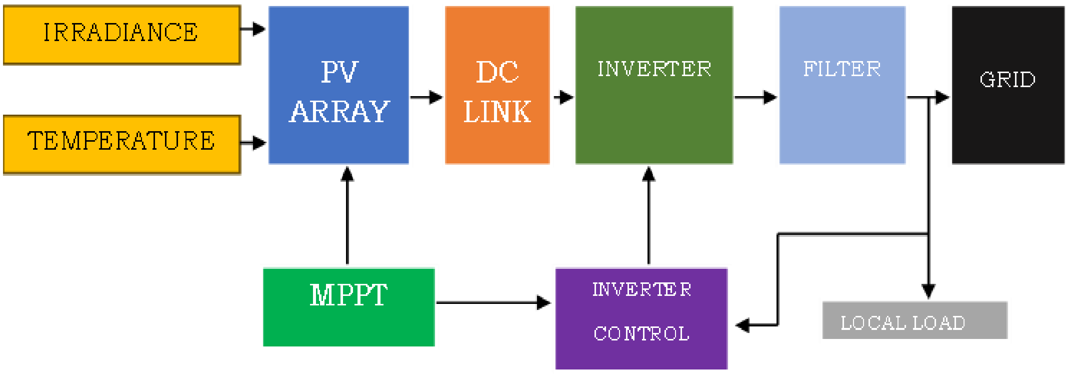

Fig 1. System Configuration

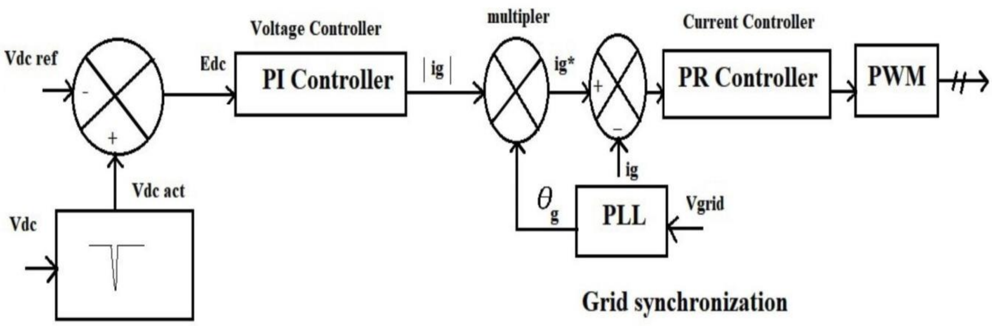

Fig.2. Control Structure

2.1 Single-Phase Grid-Connected PV Inverter Control and Operation

Figure 1 outlines the system's main components. It depicts the connection between the PV array and the inverter through the DC link, which serves to stabilize the DC voltage and mitigate fluctuations caused by occasional heavy current demands from the inverter. Subsequently, the inverter interfaces with the grid via a filter. Key inputs to the PV array include irradiance and temperature data. Within the system, the inverter plays a crucial role in converting DC voltage to AC voltage. A Maximum Power Point Tracking (MPPT) technique is incorporated, specifically, Perturbation and Observation (P&O), to determine a reference DC-link voltage (Vdc*) dependent during operation on the PV voltage. Moreover, a control mechanism, such as a proportional-integral (PI) controller utilizing a phase-locked loop (PLL), regulates the grid current's amplitude (ig), derived from the PLL, to modulate the DC-link voltage (Vdc) accordingly.

2.2. MPPT (Maximum Power Point) Operation

Perturb and Observe MPPT is used here due to its simplicity. It is the Perturb and Observe MPPT algorithm that is most widely used, and it has been around for a long time. As the flowchart in Figure illustrates, the Perturb & Observe algorithm is widely used due to its simplicity [16]. After a series of observations and perturbations, the operating point links up to the MPP. An algorithm determines the time needed to reach MPP by combining the power and voltage of time (K) with samples at a time (K-1). In positive power changes, a little voltage perturbation affects the panel's power, and the voltage perturbation continues as before. The MPP lies far from the MPP if delta power is negative, so the perturbation is reduced to approach it. Therefore, the MPP is discovered by minor perturbations of the PV curve, which amplifies the algorithm's response time. When perturbation size increases, steady-state oscillations are observed around the MPP.

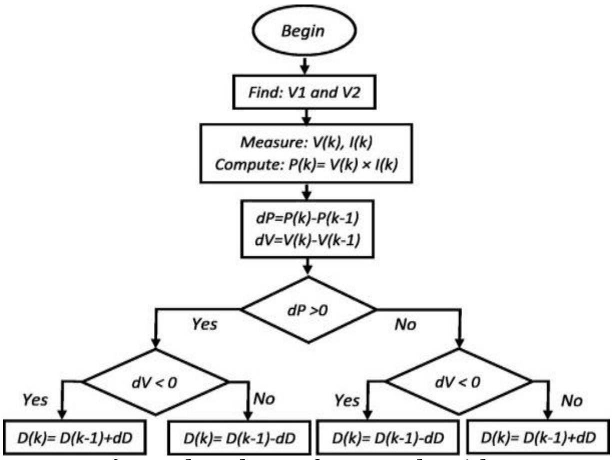

Fig.3. Flowchart of P & O Algorithm

III TYPES OF INVERTERS

3.1. (H-bridge/H4) Inverter

The DC power is converted to AC power using an H-bridge inverter with a full-bridge topology. Four controlled switches with four diodes contribute to the circuit of a full-bridge inverter, as Figure 4 below illustrates. The switching sequence of an H-bridge inverter, also known as an H4 inverter, will vary depending on the type of the output waveform and the modulation used; e.g., sinusoidal PWM, square-wave, etc. In generating a sine wave output utilizing a sinusoidal PWM method, the following is an example sequence:

Positive Half-Cycle: The output waveform during the positive half-cycle, S1, and S2 are activated to link the positive terminal of the DC input to the load. At the same time, S4 and S3 are deactivated to prevent any short circuits across the DC input.

Negative Half-Cycle: the output waveform during the negative half-cycle:

- Turning on switches S3 and S4 to connect the negative voltage of the DC input to the load.
- S1 and S2 are turned off to prevent a short circuit across the DC input.

When repeated at a high frequency, this switching sequence effectively produces a sinusoidal output waveform across the load. the magnitude of the output voltage is controlled by adjusting the duty cycle of each switch, thereby generating a sinusoidal waveform.

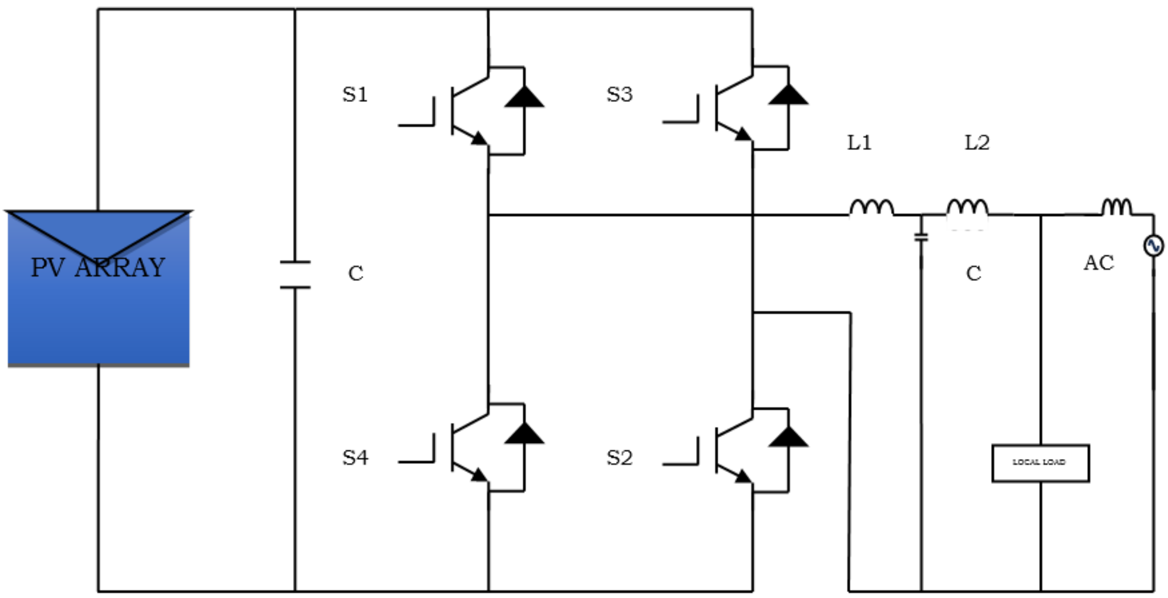

Fig 4(a) H4 inverter model circuit

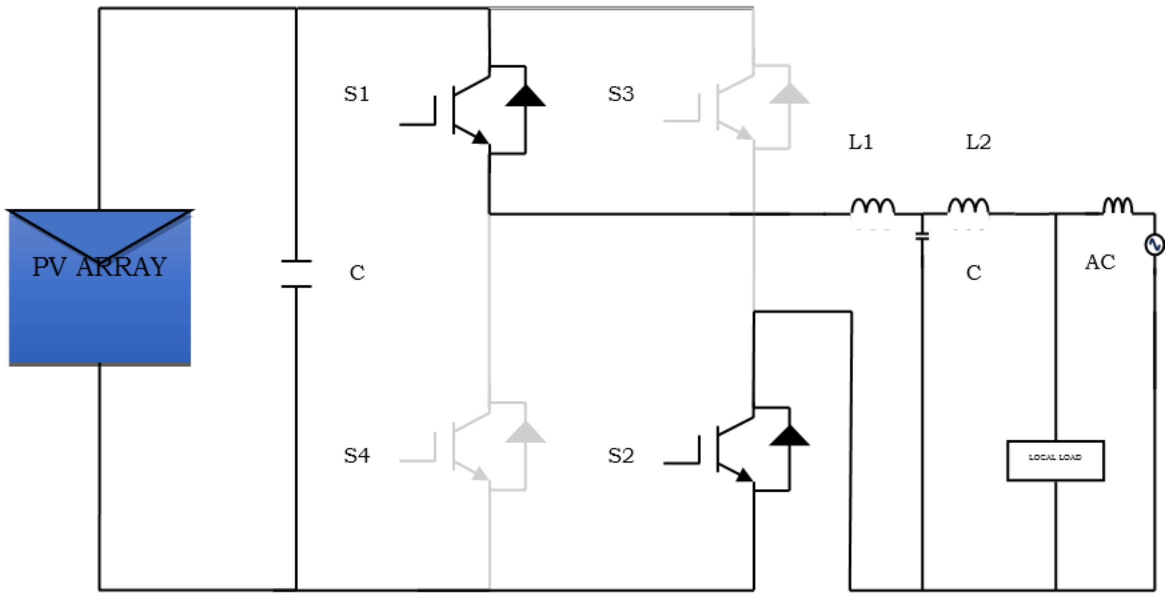

Fig 4(b) the positive half-cycle

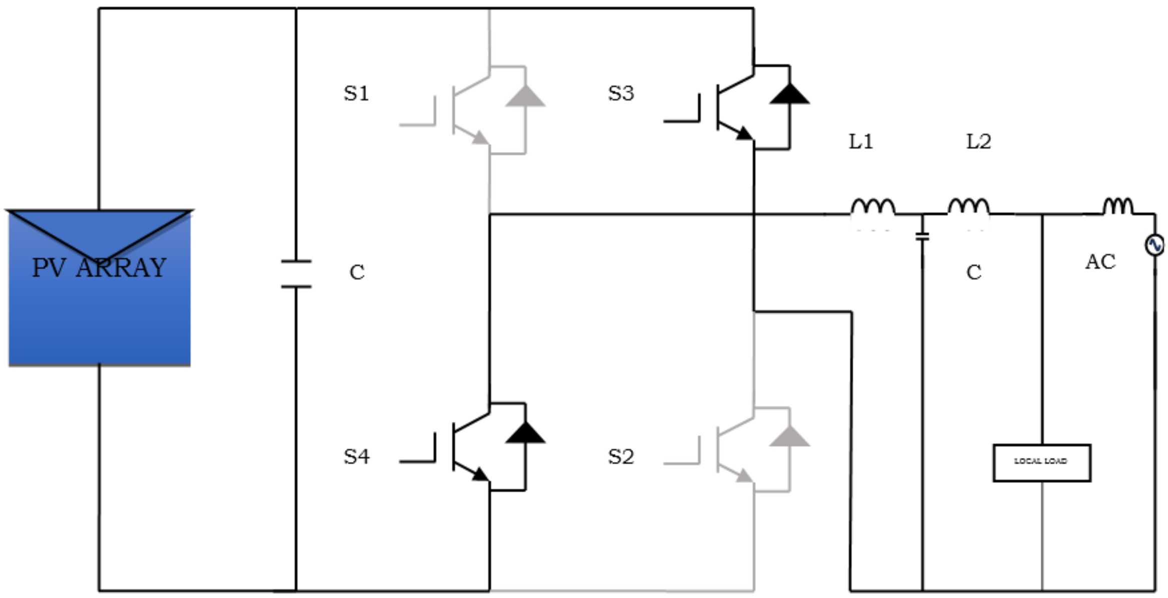

Fig 4(c) the negative the half-cycle

3.2. Proposed H6-Inverter

In Figure 5a, we present the H6 inverter setup. This configuration introduces two extra switches, S6 and S5 are incorporated into the H4 inverter design. Fundamentally in the H4 model, at the grid frequency switches S1 and S4 operate, while at the switching frequency switches S3 and S2 alternatively operate. The switches, S5 and S6, alternate between the grid frequency and switching frequency to serve as a DC which results in four distinct modes.

In the positive half cycle, switches S5, S1, S2, and S6 are triggered, as depicted in Figure 5b. In the subsequent freewheeling period, switches S2 and S6 are turned off, enabling the current to freewheel through the antiparallel diode of S3 and switch S1, as illustrated in Figure 5c.

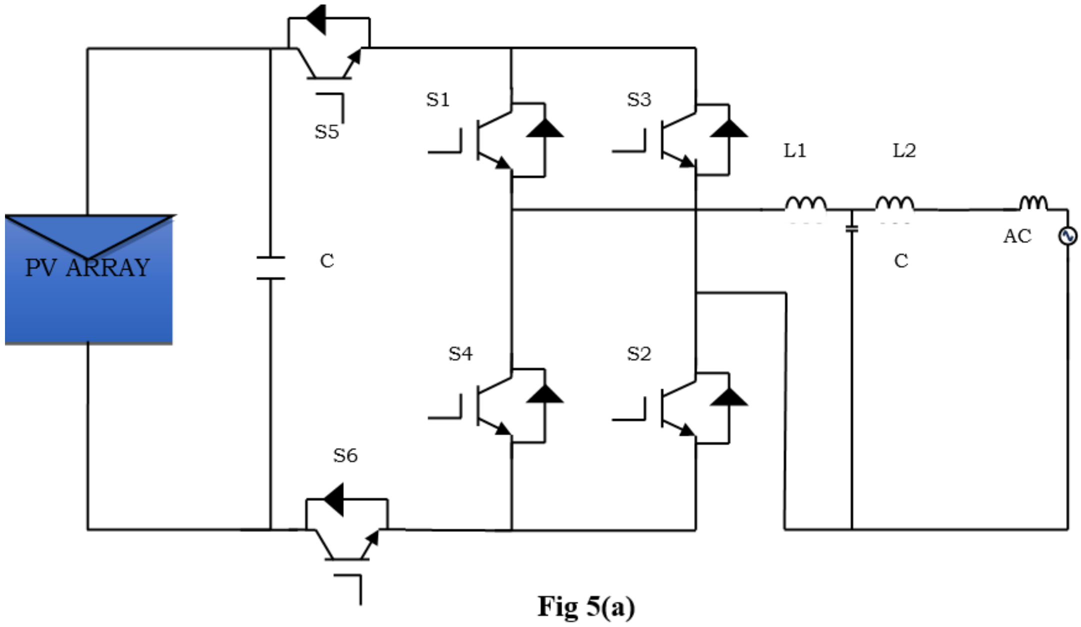

Fig 5(a)

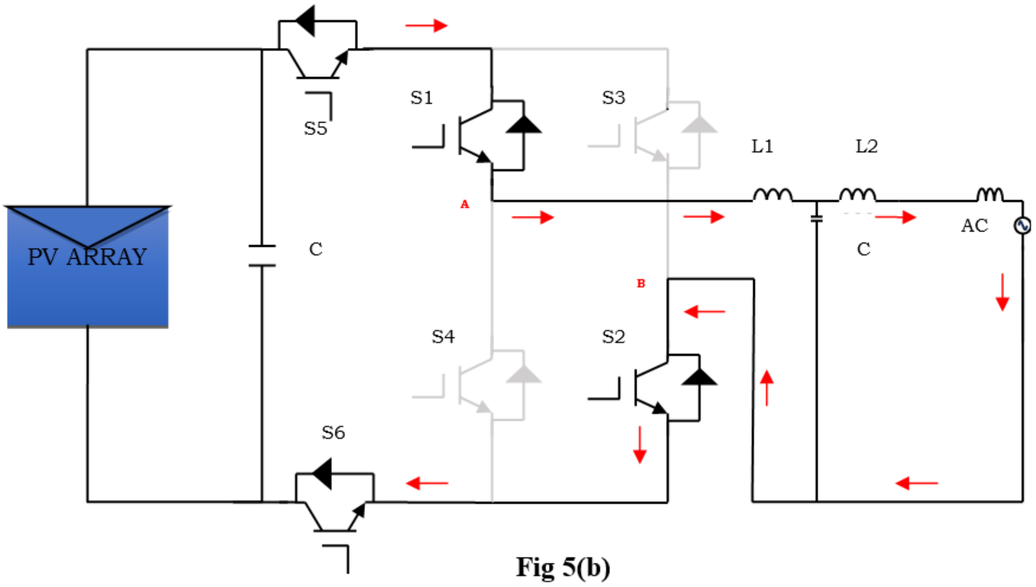

Fig 5(b)

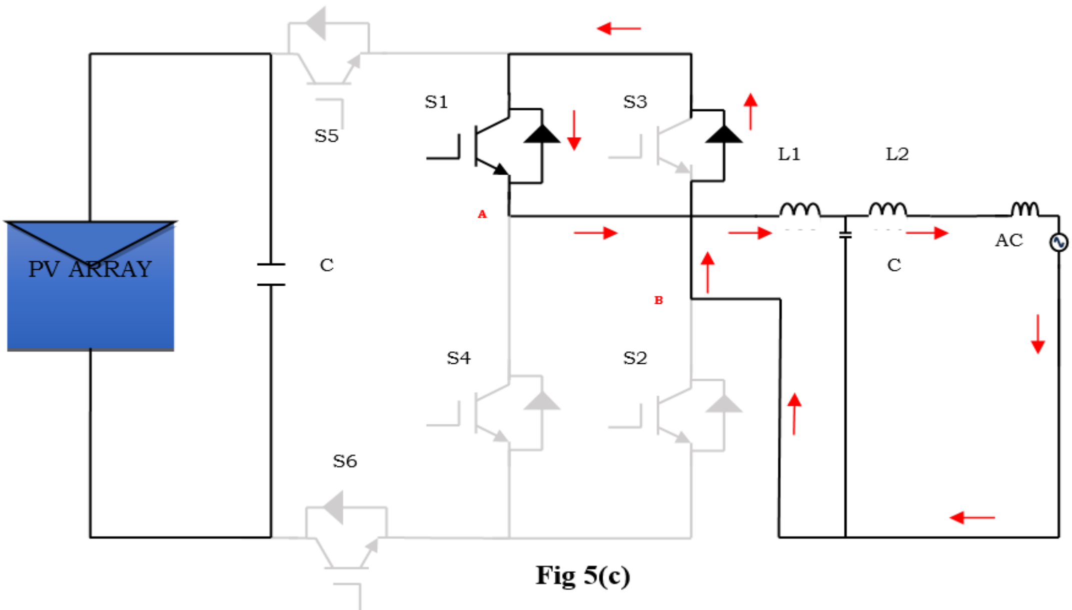

Fig 5(c)

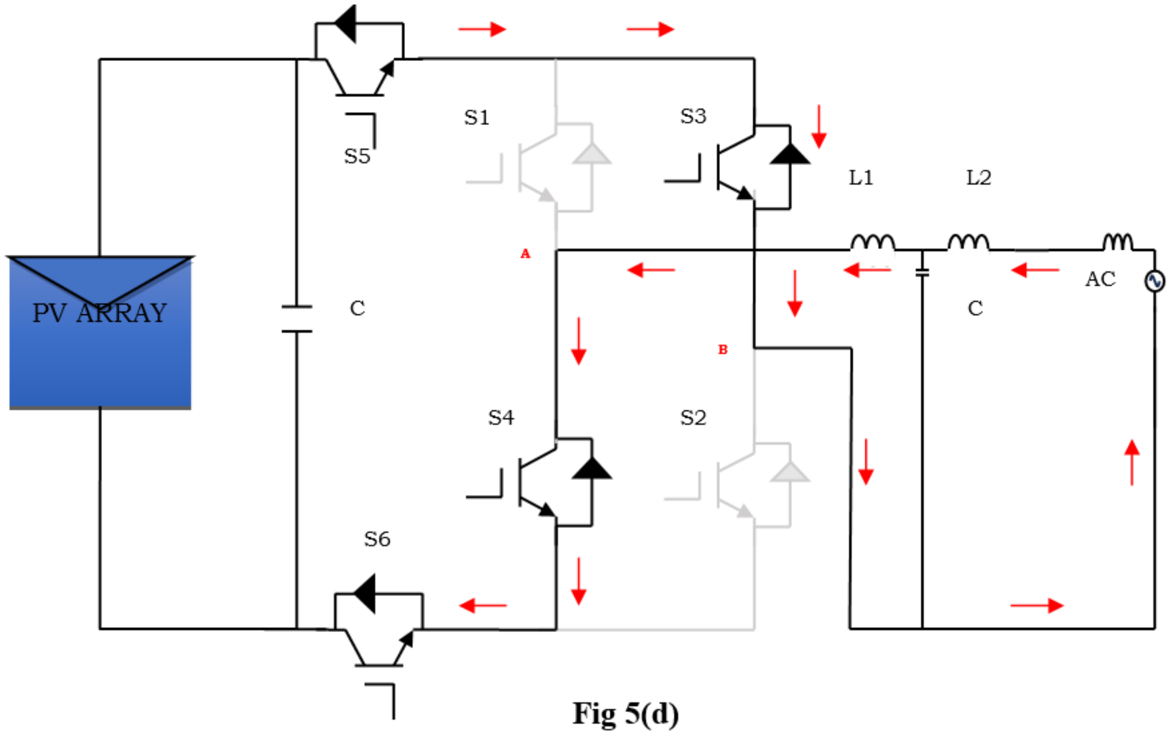

Fig 5(d)

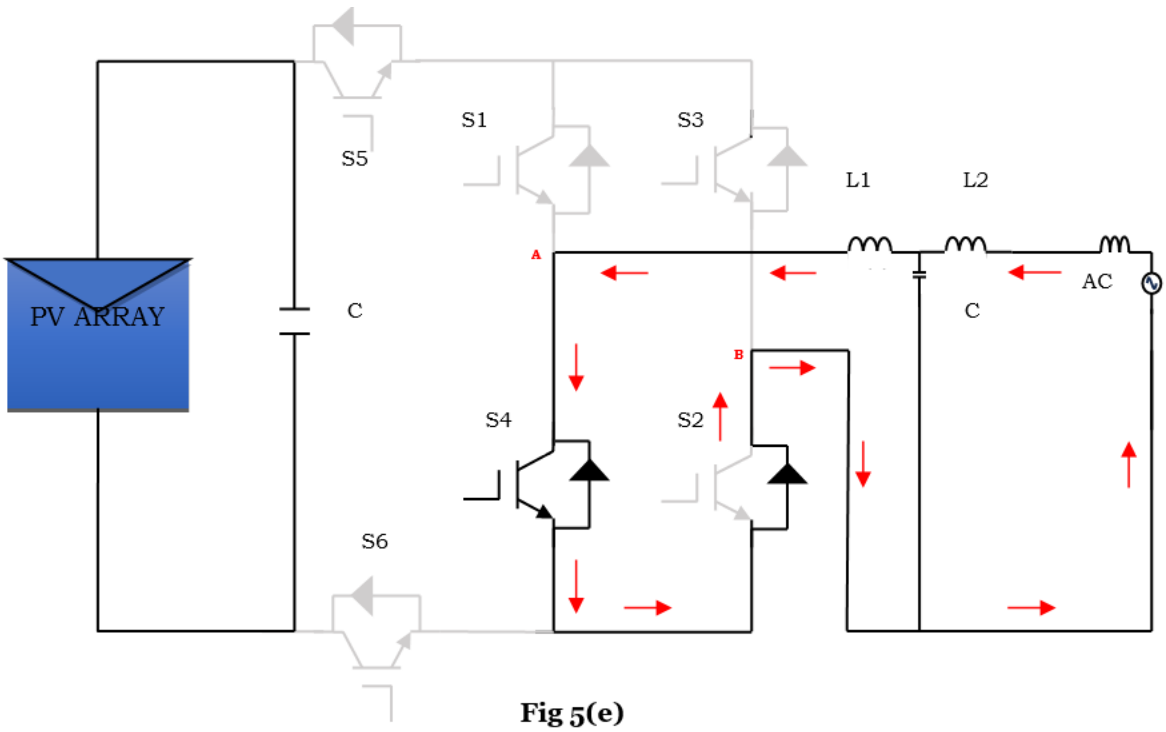

Fig 5(e)

Figure 5 showcases the H6 inverter along with its distinct operational modes:
During the negative phase of the grid voltage cycle, switches S5, S3, S4, and S6 are active, as depicted in Figure 5d. In the subsequent freewheeling period, illustrated in Figure 5e, switches S5 and S3 are switched off, allowing the current to flow through switch S4 and the antiparallel diode of S2. As a result, in both the positive and negative phases of the grid voltage cycle, four switches are engaged during active operation modes. It's worth noting that throughout all four modes, the common-mode voltage (Vcm) remains consistent at Vpv/2, effectively eradicating any leakage current.

IV Phase-locked loop (PLL)

For grid-connected operation, an inverter module integrating a phase-locked loop (PLL) is indispensable. This module utilizes the measured grid AC voltage as a reference to determine both the grid frequency and a specific phase angle for precise control of the inverter output signal. Under their closed-loop design, PLLs effectively minimize errors in both output and reference phases. As a result, the performance of the inverter is directly influenced by the operation of the PLL module [19].

Table I Grid-Connected PV System Standards and Grid Codes

Standard no	Publication Origin	THD	Power Factor
IEEE 1547 [17]	USA (IEEE)	Less than 5%	0.9 to 0.97
IEEE 929-2000 [20]	USA (IEEE)	Less than 5%	>0.85
IEC 61727 [28]	Swiss (IEC)	Less than 5%	>0.90
AS4777 [43]-[45]	Australia	Less than 5%	0.8 to 0.95
EN 61000-3-2 [22]	England	Less than 5%	NA
EREC G83 [21]	England	Less than 5%	0.95
VDE 4105 [18]	Germany	Less than 5%	0.89 to 0.95
BDEW [23]	Germany	Less than 5%	0.95
GB/T 19964-2012 [24]	China	Less than 5%	0.95
JEAC 9701-2012 [25]	Japan	Less than 5%	0.9 to 0.95

V Grid Requirements and Standards

Grid-connected photovoltaic (PV) systems must adhere to various standards set internationally and by individual countries to ensure safe and efficient integration with the grid. Below is a concise overview of key grid codes commonly regulated by major countries and associations. More detailed information can be found in [42].

Adherence to these standards is crucial for ensuring the safe and effective operation of grid-connected PV systems, and installers and operators must stay informed about and comply with relevant regulations in their respective regions. When integrating a PV panel with the grid, several parameters must be carefully managed to ensure satisfactory performance. Among these, two major ones are total harmonic distortion (THD) and power factor.

In many PV standards, the maximum allowable THD of the output current is typically limited to 5%. This restriction is aimed at enhancing power quality within distribution feeders. THD refers to the level of distortion in the electrical waveform caused by the presence of harmonics, which are multiples of the fundamental frequency. Excessive THD can lead to issues such as voltage distortion and equipment malfunction.

Additionally, the power factor is another critical parameter to consider. A low power factor can result in inefficient use of electrical infrastructure and increased losses in the system.

By adhering to standards that limit THD and emphasize a high-power factor, PV systems can contribute to improved power quality, enhance grid stability, and minimize adverse effects on electrical equipment and distribution networks.

VI Parameters of the Single-Phase Grid-Connected Photovoltaic System are shown in Table II

Table II Parameters of the 1-Phase Grid-Connected PV System

Photovoltaic Rated Power	3.5 KW
Inverter input capacitor(DC link)	C_{dc} = 1100 uF
LCL Filter	L_{inv} = 4.8 mH, C_f = 4.3 nF, L_g = 15 mH
Switching Frequency	find = 10 kHz
Controlling Sampling Frequency	f_s = 20 kHz
DC link Voltage	V_{dc} = 513 V
Grid Nominal Voltage (RMS)	V_g = 230 V
Grid Nominal Frequency	f_g = 50 Hz
Load	R=72.28 Ω L=220e-3 C=45e-6

VII Simulation Results and Discussion

7.1 Current-Voltage & Power-Voltage characteristics of Photovoltaic module

Figure 6 shows that the alternating current (Isc) increases with temperature due to its positive temperature coefficient, while the voltage (Voc) decreases as temperature rises, influenced by its negative temperature coefficient. Additionally, the power output, determined by the product of voltage and current, decreases with temperature, reflecting a negative temperature coefficient. These observations are based on standard irradiance (1000 W/m2) and a standard temperature of 25°C.

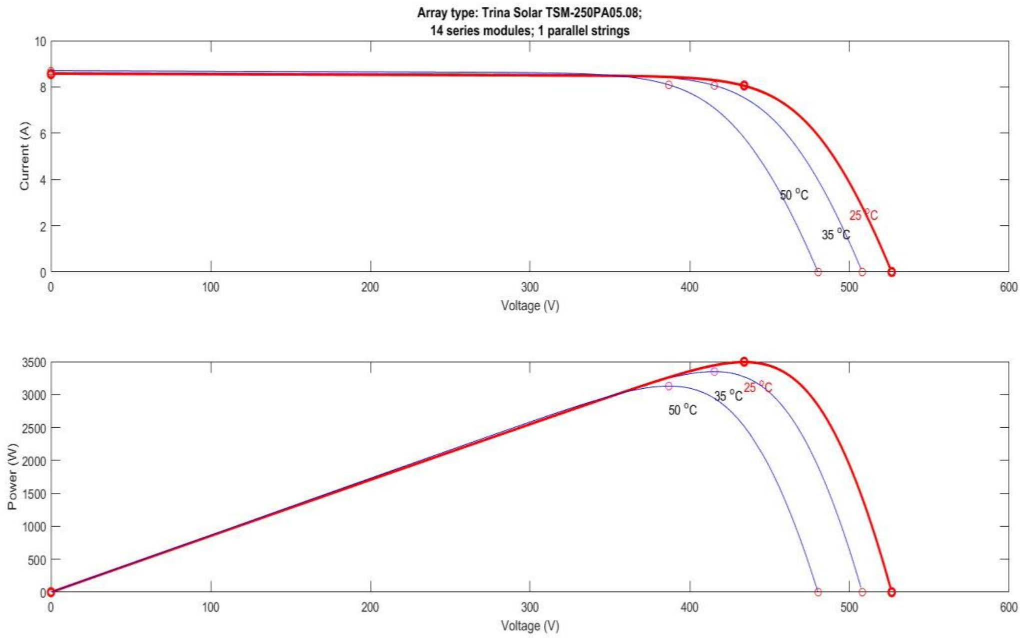

Fig 6. Current-Voltage & Power-Voltage characteristics of Photovoltaic module

7.2. Grid Voltage and Grid Current using H4 inverter in a Grid-connected Photovoltaic System

Figure 7, Upon connecting the PV system to the grid through the application of pulses to the H-Bridge inverter, harmonic distortion becomes noticeable in both the grid voltage and grid current waveforms. The presence of harmonics leads to an escalation in Distortion Power, consequently elevating the Apparent Power requirements of the system. To mitigate this challenge, improvements in the current waveform are imperative, potentially through the adoption of a novel inverter topology.

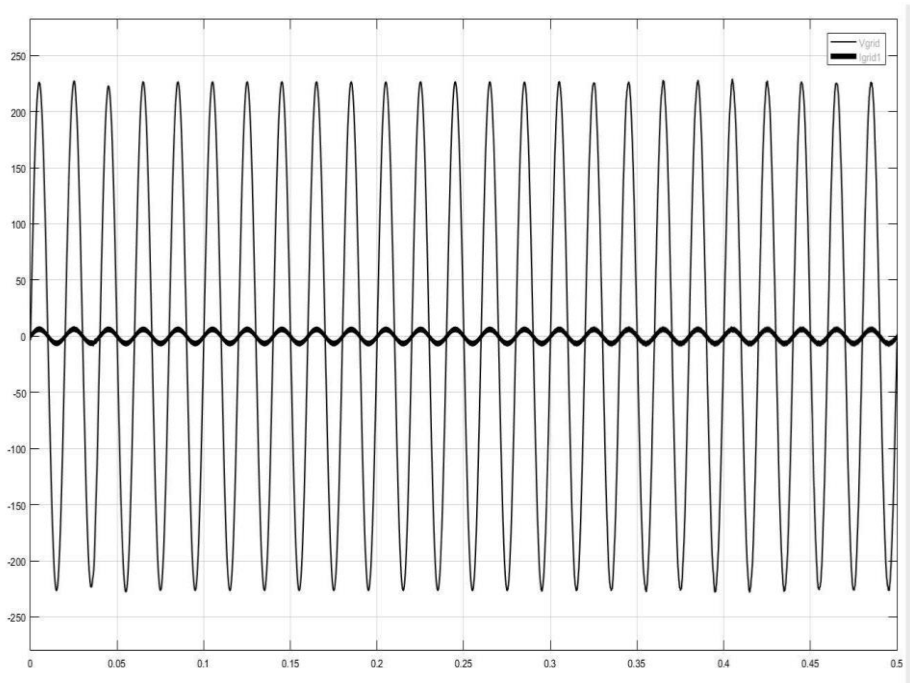

Fig 7. Grid Voltage and Grid Current using H4 inverter in a Grid-connected Photovoltaic System.

7.3. FFT (Fast Fourier Transform) spectrum for H-Bridge(H4) based Grid-connected Photovoltaic system

Figure 8 shows the FFT spectrum using an H4 inverter in a Grid-connected Photovoltaic System. The FFT spectrum for the H4 inverter gives the %THD as 7.59% at 100% loading which is not the acceptable value in grid-connected photovoltaic systems and signifies the use of other inverter topology has to be made to reduce the harmonic value.

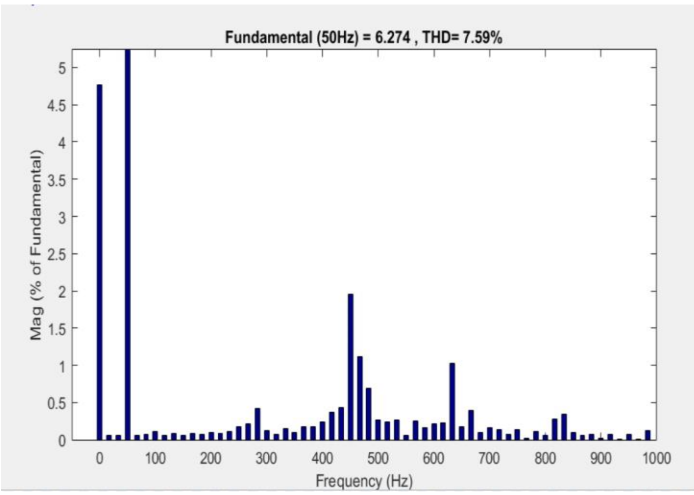

Fig 8. FFT spectrum using H4 inverter in Grid-connected Photovoltaic system

7.4. Grid Voltage and Grid Current using H6 inverter in Grid-connected Photovoltaic System

Figure 9 is the Grid Voltage and Grid Current of an H6 inverter in a Grid-connected Photovoltaic System. when the PV system is connected to the grid by giving the pulses to the H6 inverter there is less distortion or appearance of low harmonic compared to the H4 inverter. Therefore, the system has been improved by replacing the H4 inverter with the H6 inverter.

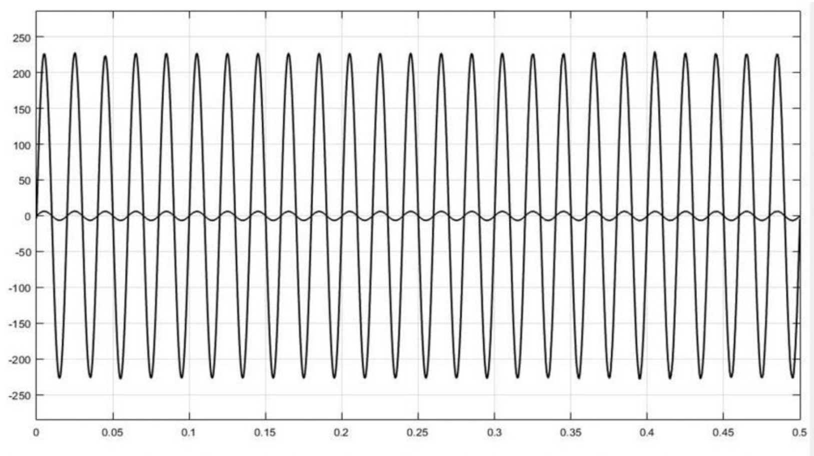

Fig.9. Grid Voltage and Grid Current using H6 inverter in Grid-connected Photovoltaic System

7.5. FFT spectrum for a grid-connected Photovoltaic system using an H6 Inverter

Below Figure 10 is the FFT spectrum of a Grid-connected Photovoltaic System using an H6 inverter. The FFT spectrum for the H6 inverter gives the %THD as 4.96% at 100% loading which is better in performance in grid-connected photovoltaic systems when compared with the conventional H4 inverter. Comparison of grid voltage, grid current, THD, and power factor at different loading conditions for H6 inverter are detailed in the IV section

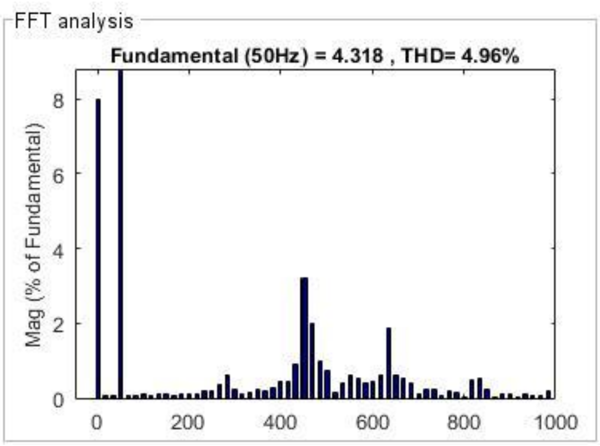

Fig.10.FFT spectrum using H6 inverter in a grid-connected Photovoltaic system

VIII Comparison of the Inverter Topologies

8.1. Table III: - Results for Grid-Connected Photovoltaic System Using H4 Inverter

The grid voltage ($V_{g\ rms}$), the grid current ($I_{g\ rms}$), the power factor(pf), and % THD for the grid current are measured at every loading condition. The simulation work for single-phase grid-connected PV systems is conducted at five different loading conditions (100%, 80%, 60%, 40%, and 20%) for both H4 and H6 inverter topologies. Grid specification in the production of voltage ranges between 220 to 240 voltages, in both topologies, the H6 inverter has a good production in voltage in comparison with the H4 inverter as the THD value is decreasing which in turn increases the apparent power and overall efficiency of the system. In the H4 inverter Efficiency decreases as the real power decreases because of the reduction of power due to the total harmonic distortion in the grid current. Grid current value represents the withstand capability for small loads in the microgrid utilization. The H6 inverter topology has high reliability when compared with the H4 inverter in the context of supplying power to the load.

Load Variations (%)	Grid Voltage (Vg)	Grid Current (Ig)	Power Factor (pf)	% THD for grid current
100	228.3	3.237	0.989	7.59
80	228.4	3.965	0.989	6.72
60	228.5	5.239	0.991	5.92
40	227.4	7.797	0.992	4.25
20	228.1	14.54	0.992	3.25

8.2. Table IV Results for Grid-Connected Photovoltaic System Using H6 Inverter

Load Variations (%)	Grid Voltage (Vg)	Grid Current (Ig)	Power Factor	% THD for grid current
100	229	3.27	0.992	4.96
80	228.4	3.96	0.994	4.62
60	228.4	5.239	0.995	3.78
40	228.6	7.824	0.996	2.59
20	228.9	14.62	0.997	1.19

8.3. Power Factor Comparison Between H4 and H6 Inverter

Figure 11 is the power factor comparison of a Grid-connected Photovoltaic System using H4 and H6 inverters. The power factor defines whether the voltage is in phase with the current or not. From the above figure, we can say that the grid-connected system using the h6 inverter shows better performance when compared with the conventional h4 inverter in grid-connected photovoltaic systems.

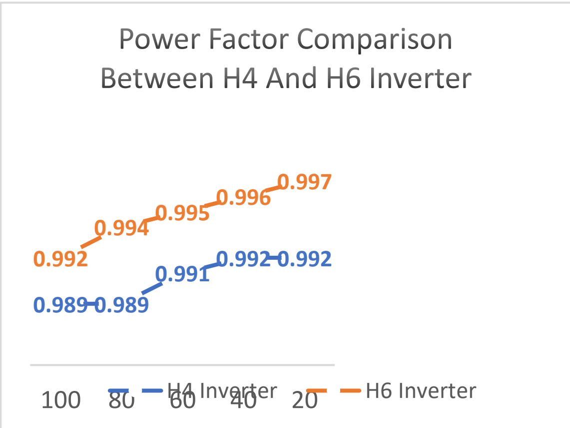

Fig11. Power Factor Comparison between H4 and H6 Inverter

The power factor also signifies the efficiency of the system. If we refer to the causes of the low power factor one of the fundamental causes is the presence of harmonic current. so, the presence of harmonics directly impacts the reduction of the power factor as seen in the graph.

8.4 THD Comparison Between H4 and H6 Inverter

figure 12 is the Thd comparison of a Grid-connected Photovoltaic System using H4 and H6 inverters. From the above figure, the grid-connected system using the h6 inverter performs better in terms of Thd when compared with the conventional H4 inverter in grid-connected photovoltaic systems. The Thd signifies the efficiency of the system. The presence of harmonics directly impacts the reduction of the power factor. In the proposed model the H6 inverter is used in the grid-connected photovoltaic system which reduces the harmonics.

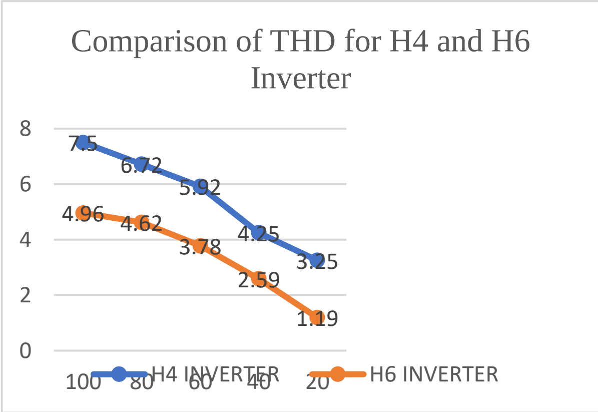

Fig12. Comparison of THD for H4 and H6 Inverter

From the graph when the load is 20% the percentage of difference in the value between H4 and H6 is 36.6% when the load is 100% the percentage of difference in the value between H4 and H6 is 59.4%, therefore when the load is increasing from 20% to 100 % the difference of the value of THD between H4 and H6 is 22.8% which emphasis the necessity of using H6 inverter in a grid-connected photovoltaic system.

IX Conclusion

When Photovoltaic systems are connected to the grid, there are several challenges to consider. One of the challenges, specifically with the large-scale use of PV systems, is harmonics in PV systems. This paper investigates the use of inverters to reduce harmonics and improvement in the power factor in grid-connected PV systems.
MATLAB/Simulink was used to create a single-phase grid-connected PV system for both the H4 and H6 inverters. Total Harmonic Distortion was utilized as the performance metric in this comparison (THD). This study presents the simulation results using the Harmonic spectrum. The H4 inverter has a percent THD of 7.59 percent for single-phase grid-connected Photovoltaic systems during 100 % loading, but the H6 inverter has a percent THD of 4.96 percent for 100% loading. There is a significant improvement in the power factor using the H6 inverter When compared to a system utilizing the H4 inverter. The proposed system's reduction of %THD and enhancement of the power factor highlight its importance in practical usage.

X REFERENCES

1. M. E. Ropp, M. Begovic, and A. Rohatgi, “Prevention of islanding in grid-connected photovoltaic systems,” Prog. Photovoltaics, vol. 7, pp.39–59, 1999.
2. A. Mansoor, W. M. Grady, P. T. Staats, R. S. Thallam, M. T. Doyle, and M. J. Samotyj, “Predicting the net harmonic currents produced by large numbers of distributed single-phase computer loads,” Inst. Elect. Eng. Trans. Power Dist., vol. 10, no. 4, pp. 2001–2006, 1995.
3. E. F. El-Saadany and M. M. A. Salama, “Reduction of the net harmonic current by single-phase nonlinear loads due to attenuation and diversity effects,” Int. J. Elec. Power Energy Syst., vol. 20, no. 4, pp. 259–268,1998.
4. IEEE Draft Standard for Interconnecting Distributed Resources with Electric Power Systems, IEEE P1547/D10.
5. “Recommendations for the Connection of Small-Scale Embedded Generators (Up to 16 A per Phase) in Parallel with Public Low☐Voltage Distribution Networks,” Electricity Association, London, U.K., 2002.
6. Tekai Eddine Khalil Zidane, Ali Saleh Aziz, Younes Zahraoui, Hossam Kotb, Kareem M. Aboras, Kitmo, And Yosef Berhan Jember “Grid-Connected Solar PV Power Plants Optimization: A Review” IEEE Access (Volume: 11), IEEE, 28 July 2023.
7. M. Jagabar Sathik, (Senior Member, IEEE), Mahmoud F. Elmorshedy, (Senior Member, IEEE), And Dhafer J. Almakhles, (Senior Member, IEEE) “A New Boost Topology Seven-Level Inverter of High Voltage Gain Ability and Continuous Input Current with MPPT for PV Grid Integration” IEEE Access (Volume: 11), IEEE, 05 December 2023.
8. Yongheng Yang, Member, IEEE, Keliang Zhou, Senior Member, IEEE, And Frede Blaabjerg, Fellow, IEEE “Current Harmonics from Single-Phase Grid-Connected Inverters—Examination and Suppression” IEEE Journal of Emerging and Selected Topics in Power Electronics, Vol. 4, No. 1, March 2016.

9. Tripura Pidikiti, Sheedevi, Gireesha B, *Mopidevi Subbarao and V. B Murali Krishna, "Design and Control of Takagi-Sugeno-Kang Fuzzy Controller based Inverter for Power Quality Improvement in Grid-tied PV Systems" Measurement: Sensors, Vol. 25, 100638, 2023, Elsevier, ISSN: 2665-9174, DOI: https://doi.org/10.1016/j.measen.2022.100638
10. Rajesh Cheruku, Jae Hong Kim, VB Murali Krishna, P Periyat, Sarathbabu Duvvuri SSSR, "Photo-electrodes decorated with carbon quantum dots: Efficient dye-sensitized solar cells", Results in Engineering, Volume 20, 101611, Dec 2023. DOI: https://doi.org/10.1016/j.rineng.2023.101611
11. Yongheng Yang, Student Member, IEEE, Keliang Zhou, Senior Member, IEEE, Huai Wang, Member, IEEE, Frede Blaabjerg, Fellow, IEEE, Danwei Wang, Senior Member, IEEE, And Bin Zhang, Senior Member, IEEE "Frequency Adaptive Selective Harmonic Control for Grid-Connected Inverters" IEEE Transactions on Power Electronics, Vol. 30, No. 7, July 2015.
12. Y. Yang and F. Blaabjerg, "Overview of single-phase grid-connected photovoltaic systems," Elect. Power Compon. Syst., vol: 43, no. 12, pp. 1352– 1363, Jul. 2015.
13. DKE Deutsche Kommission Elektrotechnik Elektronik Informationstech- nik im DIN und VDE, Deutsche Kommission Elektrotechnik, Frankfurt Germany, DIN V VDE V 0126-1-1, 2006.
14. W. Li, Y. Gu, H. Luo, W. Cui, X. He, and C. Xia, "Topology review and derivation methodology of single-phase Transformerless photovoltaic inverters for leakage current suppression," IEEE Trans. Ind. Electron., vol. 62, no. 7, pp. 4537–4552, Jul. 2015.
15. L. Zhang, K. Sun, Y. Xing, and M. Xing, "H6 Transformerless full-bridge PV grid-tied inverters," IEEE Trans. Power Electron., vol. 29, no. 3, pp. 1229–1238, Mar. 2014.
16. D. Meneses, F. Blaabjerg, O. Garcia, and J. A. Cobos, "Review and comparison for step-up Transformerless topologies for photovoltaic ac-module application," IEEE Trans. Power Electron., vol. 28, no. 6, pp. 2649–2663, Jun. 2013.
17. IEEE Standard Conformance Test Procedures for Equipment Interconnecting Distributed Resources with Electric Power Systems, Standard 1547.1-2005, 2005, pp. 1–54.
18. Power Generation Systems Connected to the Low-Voltage Distribution Network-Technical Minimum Requirements for the Connection to and Parallel Operation with Low-Voltage Distribution Networks, document VDE-AR-N 4105-2011, Association for Electrical, Electronic & Information Technologies (VDE), 2011.
19. D. Barater, G. Buticchi, A. S. Crinto, G. Franceschini, and E. Lorenzani, "Unipolar PWM strategy for Transformerless PV grid-connected converters," IEEE Trans. Energy Convers., vol. 27, no. 4, pp. 835–843, Dec. 2012.
20. Recommended Practice for Utility Interface of Photovoltaic Systems, IEEE Standard 929-2000, 2000.
21. Recommendations for the Connection of Type Tested Small-Scale Embedded Generators (Up to 16A Per Phase) in Parallel with Low-Voltage Distribution Systems, Energy Networks Association (ENA), document Engineering Rec. G83 2-2012, 2012.
22. European Power Supply Manufacturers Association, Guidelines to the Standard EN 61000-3-2, 2010.
23. Guideline for Generating Plants' Connection to and Parallel Operation with the Medium-Voltage Network, BDEW, Berlin, Germany, 2008.
24. Technical Requirements for Connecting Photovoltaic Power Station to Power System, document GB/T 19964-2012, Standardization, Administration of the P.R.C., 2012.
25. Grid-Interconnection Code, the Japan Electric Association, document JEAC 9701-2012, 2012.
26. D. Barater, E. Lorenzani, C. Concari, G. Franceschini, and G. Buticchi, "Recent advances in single-phase Transformerless photovoltaic inverters," IET Renewable Power Gener., vol. 10, no. 2, pp. 260–273, Aug. 2015.
27. H. Xiao, S. Xie, Y. Chen, and R. Huang, "An optimized Transformerless photovoltaic grid-connected inverter," IEEE Trans. Ind. Electron., vol. 58, no. 5, pp. 1887–1895, May 2011.
28. H. F. Xiao, K. Lan, and L. Zhang, "A quasi-unipolar SPWM full-bridge Transformerless PV grid-connected inverter with constant common-mode voltage," IEEE Trans. Power Electron., vol. 30, no. 6, pp. 3122–3132, Jun. 2015.
29. Characteristics of the Utility Interface for Photovoltaic (PV) Systems, document IEC 61727 CDV (Committee Draft for Vote), 2002.
30. B. Yang, W. Li, Y. Gu, W. Cui, and X. He, "Improved Transformerless inverter with common-mode leakage current elimination for a photovoltaic grid-connected power system," IEEE Trans. Power Electron., vol. 27, no. 2, pp. 752–762, Feb. 2012.
31. G. Infield, P. Onions, A. D. Simmons, and G. A. Smith, "Power quality from multiple grid-connected single-phase inverters," IEEE Transactions on Power Delivery vol. 19, no. 4, pp. 1983–1989, October. 2004. DOI: 10.1109/TPWRD.2004.829950.
32. F. Katiraei and J. R. Aguero, "Solar PV integration challenges," IEEE Power and Energy Magazine, Volume: 9, Issue: 3, May-June 2011, pp. 62–71, May 2011. DOI: 10.1109/MPE.2011.940579.
33. F. Blaabjerg, Y. Yang, D. Yang, and X. Wang, "Distributed power- generation systems and protection," Proc. IEEE, volume. 105, no. 7, pp. 1311– 1331, July. 2017.

34. M. Ciobotaru "Reliable grid condition detection and control of single-phase distributed power generation systems,", Ph.D. dissertation, Dept. Energy Technol., Aalborg, Aalborg Univ., Denmark, 2009.
35. Y. Du, D. D.-C. Lu, G. James, and D. J. Cornforth, "Modeling and analysis of current harmonic distortion from grid-connected PV inverters under different operating conditions," Sol. Energy, volume. 94, pp. 182–194, August. 013.https://doi.org/10.1016/j.solener.2013.05.010
36. Sosa, J.M.; Escobar, G.; Martinez-Rodriguez, P.R.; Vazquez, G.; Juarez, M.A.; Diosdado, M." Comparative evaluation of L and LCL filters in Transformerless grid-tied converters for active power injection,", in 2014 IEEE International Autumn Meeting on Power, Electronics, and Computing (ROPEC), November. 2014, pp.1-6, 5-7, DOI: 10.1109/ROPEC.2014.7036284.
37. Sumant Kumar Dalai; Rojalin Sahu; Chandra Sekhar Tripathy, "Harmonic Mitigation in Single-Phase Grid Connected Photovoltaic System Using SPWM Inverter",2020 International Conference on Computational Intelligence for Smart Power System and Sustainable Energy (CISPSSE), IEEE, DOI: 10.1109/CISPSSE49931.2020.9212280.
38. Jose M. Sosa; Panfilo R. Martinez-Rodriguez; Gerardo Escobar; Gerardo Vazquez; Andres A. Valdez-Fernandez, "Analysis and Validation for an Inverter-side Current Controller in LCL Grid-connected Power Systems", Journal of Modern Power Systems and Clean Energy (Volume: 8, Issue: 2, March 2020), DOI: 10.35833/MPCE.2018.000505.
39. Manish Bhardwaj; Shamim Choudhury; Vieri Xue; Bilal Akin "Online LCL filter compensation using embedded FRA," in 2014 IEEE Applied Power Electronics Conference and Exposition - APEC 2014, March 2014, pp.3186-3191, DOI: 10.1109/APEC.2014.6803761.
40. Controller in LCL Grid-connected Power Systems", Journal of Modern Power Systems and Clean Energy (Volume: 8, Issue: 2, March 2020), DOI: 10.35833/MPCE.2018.000505.
41. Manish Bhardwaj; Shamim Choudhury; Vieri Xue; Bilal Akin "Online LCL filter compensation using embedded FRA," in 2014 IEEE Applied Power Electronics Conference and Exposition - APEC 2014, March 2014, pp.3186-3191, DOI: 10.1109/APEC.2014.6803761.
42. Y.-K. Wu, J.-H. Lin, and H.-J. Lin, "Standards and guidelines for grid-connected photovoltaic generation systems: A review and comparison," IEEE Trans. Ind. Appl., vol. 53, no. 4, pp. 3205–3216, Jul./Aug. 2017.
43. Grid Connection of Energy Systems via Inverters Part 1: Installation Requirements, Council of Standards Australia, document AS 4777.1- 2005, 2005.
44. Grid Connection of Energy Systems via Inverters Part 2: Inverter Requirements, Council of Standards Australia, document AS 4777.2- 2005, 2005.
45. Grid Connection of Energy Systems via Inverters Part 3: Grid Protection Requirements, Council of Standards Australia, document AS 4777.3-2005, 2005.